# Influence of optical coherence on the electron spin in singly charged InP quantum dots excited by resonant laser pulses



doi: 10.1103/PhysRevB.85.235320

# Influence of optical coherence on the electron spin in singly charged InP quantum dots excited by resonant laser pulses

Shinichi Tomimoto, Keisuke Kawana, Akira Murakami, and Yasuaki Masumoto
*Faculty of Pure and Applied Sciences, University of Tsukuba, Tsukuba 305-8571, Japan*
(Received 9 December 2011; revised manuscript received 14 May 2012; published 26 June 2012)

We have experimentally studied the spin dynamics of excitons, electrons, and trions in charge-tunable InP/InGaP quantum dots (QDs) excited by picosecond resonant laser pulses by observing the time-resolved Kerr rotation. In singly charged QDs, inversion of the spin polarization direction of doped electrons is found to be caused simply by variation in the pulse intensity, which is accompanied by an abrupt change of the spin coherence time. This phenomenon is reproduced by density-matrix calculations allowing for the reaction on the QD electron-trion four-level system during its coherent radiation emission. This result means that the optical coherence is another critical factor affecting electron spin coherence.

DOI: 10.1103/PhysRevB.85.235320 PACS number(s): 78.67.Hc, 72.25.Fe, 78.47.D−

## I. INTRODUCTION

Singly charged quantum dots (QDs), which have one residual electron on each, can balance two competing features as spin qubits,[1,2] i.e., optical operability[3,4] and long-lived spin coherence[5] which is free from the finite lifetimes of the relevant optically excited states.[6] The high-fidelity initialization[7] and ultrafast control[8,9] of the electron spin demonstrated in a single QD will lead the way to the practical qubit operations. The spin and optical properties of singly charged QDs are well illustrated by a four-level system[10] consisting of two electron (ground) and two trion (excited) levels. It is shown in Fig. 1. In this system, we can define two types of quantum coherence. One is the spin coherence which is defined between the electron (trion) spin levels $|x\rangle$,$|\bar{x}\rangle$ ($|Tx\rangle$,$|T\bar{x}\rangle$). The other is the optical coherence between the ground (electron) and optically excited (trion) states which are connected by $\pi_x$ and $\pi_y$ transitions as indicated in Fig. 1(a). In general, these two types of coherence are treated independently, except in the presence of an external light field, because their characteristic frequencies differ by more than three orders of magnitude under the usual experimental conditions. Thus the interplay between them has been left unexplored, although the optical coherence is known to have a significantly long lifetime in QDs.[11]

Here we report the observation of electron spin dynamics critically influenced by the optical coherence. We have experimentally studied the spin dynamics of excitons, electrons, and trions in charge-tunable InP/InGaP QDs excited by picosecond resonant light pulses by observing the time-resolved Kerr rotation (TRKR). In singly charged QDs, it is found that the spin polarization direction of the single electrons is inverted simply by varying the pulse intensity, and the spin coherence time abruptly changes on the occurrence of the inversion. This phenomenon is well reproduced by numerical simulations allowing for the reaction on the four-level system during its coherent radiation emission. This manifests the critical role played by the optical coherence in the electron spin dynamics.

## II. EXPERIMENT

The samples investigated here are charge-tunable InP QDs.[12,13] The self-assembled QDs are embedded in $In_{0.5}Ga_{0.5}P$ barriers grown on an $n^+$-GaAs substrate. In this sample, an ensemble of QDs singly charged ($V_B = -0.175$ V) or neutral (−0.8 V) on average can be prepared by applying an appropriate voltage bias $V_B$ along the crystal growth axis $z$. This is mounted in a magneto-optical cryostat with sample temperature of $T = 5$ K. The spin dynamics was observed by TRKR measurements in transverse magnetic fields $B \parallel x$ (Voigt geometry).[2] Degenerate pump and probe pulses traveling along $-z$ are obtained from a mode-locked Ti:sapphire laser (repetition rate 82 MHz). They have a pulse width of about 2 ps, which determines the time resolution of the measurement. The pump pulse is circularly polarized, and focused onto the sample (spot diameter 250 $\mu$m) after being optically chopped at 210 Hz.

## III. RESULTS AND DISCUSSION

### A. Spin properties of excitons, single electrons, and trions in InP QDs

Figure 2(a) shows the time dependence of Kerr rotation for neutral QDs ($V_B = -0.8$ V) at four different magnetic fields $B$. It is a superposition of two oscillations corresponding to the peaks in the fast-Fourier-transform (FFT) spectrum of Fig. 2(c) ($B = 8$ T). The lower-frequency component with a period of about 21 ps at $B = 8$ T comes from the spin precession of electrons in the GaAs substrate. It is not important here. Meanwhile, the higher-frequency component originates from the spin beat of excitons photogenerated in the neutral QDs. It is seen as the short-lived oscillation in Fig. 2(a), which has a period of 5.9 ps at $B = 8$ T and decays in about 50 ps. The assignment of these components is supported by the spectral characteristics shown in Fig. 3(a) where the FFT peak amplitudes at $B = 6$ T are plotted as functions of the photon energy of the pump and probe. The exciton component presents clear resonance at the photoluminescence (PL) band of the QDs, unlike the substrate component. The corresponding peak frequencies shown in Fig. 3(c) scarcely depend on the photon energy. The open circles (black) in Fig. 3(e) show the magnetic-field dependence of the frequency of the exciton component. It deviates from a simple linear relation at fields lower than 4 T. These data are well fitted by the dashed line which presents the energy splitting between two exciton spin

 

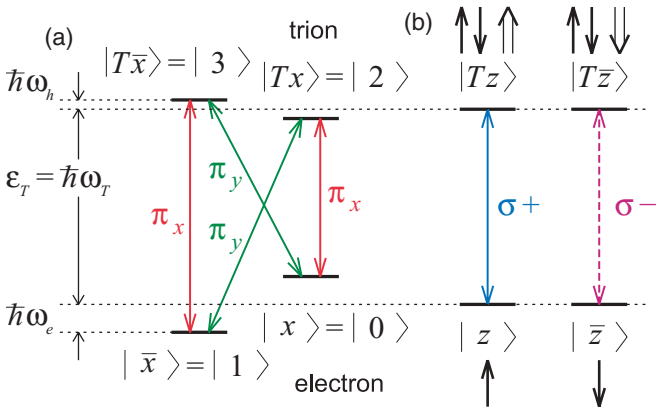


FIG. 1. (Color online) Schematic energy diagrams of the electron-trion four-level system in a magnetic field $B \parallel x$ which is perpendicular to the QD growth axis $z$. The pump pulse is assumed to be traveling along $-z$ (Voigt geometry). (a) Energy eigenstates consisting of two electron spin states $|x\rangle = |0\rangle$, $|\bar{x}\rangle = |1\rangle$ and two trion (negatively charged exciton) spin states $|Tx\rangle = |2\rangle$, $|T\bar{x}\rangle = |3\rangle$. The Zeeman splittings are $2\hbar\omega_e$ and $2\hbar\omega_h$ for the electron and trion, respectively. (b) The same system shown in the basis of the $z$ axis. The arrows $\uparrow$ and $\Uparrow$ represent electron and hole spins, respectively.

states in transverse fields $B$. It is given by $\hbar\Omega = \sqrt{(\hbar\omega)^2 + \delta^2}$, where $\hbar\omega = 2\hbar\omega_e = g_e\mu_B B$ is the electron Zeeman splitting ($\mu_B$ is the Bohr magneton), and $\delta = 170$ $\mu$eV is the isotropic electron-hole exchange.[14,15]

The electron $g$ factor, $|g_e| = 1.52$, is independently determined from the data for singly charged QDs ($V_B = -0.175$ V) in Fig. 2(b). Here the time dependence of Kerr rotation consists of oscillation components corresponding to the FFT peaks in Fig. 2(d) ($B = 6$ T). One of them is the substrate component, which is seen as the slow oscillation with a period of about 180 ps at $B = 1$ T. Another pronounced component with a higher frequency originates from the single electrons doped in the QDs. This has a period of 47 ps at 1 T, and has a much longer lifetime (about 2 ns) than that of the exciton component. The oscillation reflects the spin precession of the single electrons whose spins are polarized by the pump pulse resonant with the electron-trion (negatively charged exciton $X^-$) transition. As seen in Fig. 3(b) ($B = 2$ T), this component also shows resonance at the PL band of QDs, in which it is different from the substrate component. The oscillation frequency hardly depends on the photon energy [Fig. 3(d)]. In Fig. 3(e), the frequencies of the electron and substrate components ($V_B = -0.175$ V) are shown by open triangles (blue) and squares (black), respectively. They exhibit simple linear dependence on the magnetic field, which corresponds to the $g$ factors $|g_e| = 1.52$ for the single electrons in the QDs,[16] and $|g_{sub}| = 0.40$ for the substrate components. The latter agrees reasonably well with the known value in bulk GaAs ($-0.44$).[17]

For the singly charged QDs ($V_B = -0.175$ V), we have found a third component which originates from the spin coherence in the photoexcited states, i.e., the trions. This appears as the FFT peak at the lowest frequency (0.0057 THz) in Fig. 2(d) ($B = 6$ T). The slow oscillation corresponding to this peak can be clearly seen in the data of Fig. 2(e). These data are obtained by removing the higher-frequency

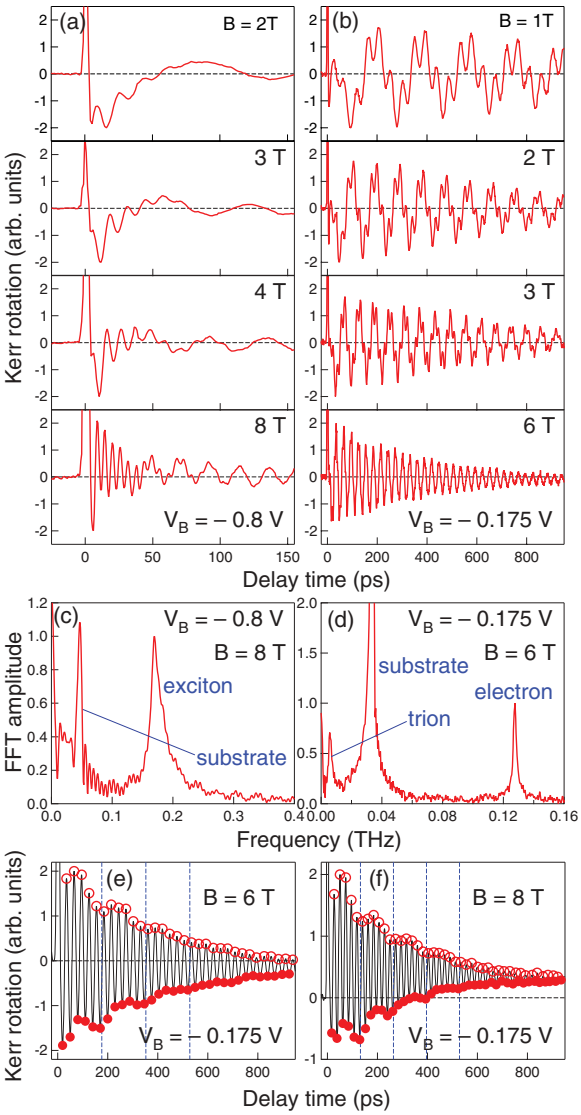


FIG. 2. (Color online) Time dependence of Kerr rotation at $V_B =$ (a) $-0.8$ V and (b) $-0.175$ V. (c), (d) FFT spectra. (e), (f) Time dependence of TRKR after removing the electron component. (Pump intensity $I \sim 10$ mW; pump-probe photon energy $E_p = 1.74$ eV.)

electron component from the data of Fig. 2(b) ($B = 6$ T) by numerical smoothing. Here the oscillation peaks and troughs (coming from the substrate component) are marked by open and filled circles (red), respectively. These marks manifest a slow oscillation which decays in a few periods. By the same treatment, we obtain the data at $B = 8$ T in Fig. 2(f), where the oscillation is a little faster. The frequency of this component is shown by filled triangles (red) in Fig. 3(e). It also has linear dependence on the magnetic field with the $g$ factor of $|g_h| = 0.068$. The equally spaced broken lines in Figs. 2(e) and 2(f) show the oscillation periods given by this value of $g_h$. As it is close to the known heavy-hole $g$ factor in the QDs ($\sim$0.1),[13,18] we ascribe the slow oscillation to the spin precession of the heavy hole in the trion. It is formed by the photoexcitation of the singly charged QDs (Fig. 1). The other part of the trion, a spin-singlet pair of electrons, does not contribute to TRKR. The fast oscillation damping seen in Figs. 2(e) and 2(f) reflects the trion recombination lifetime,

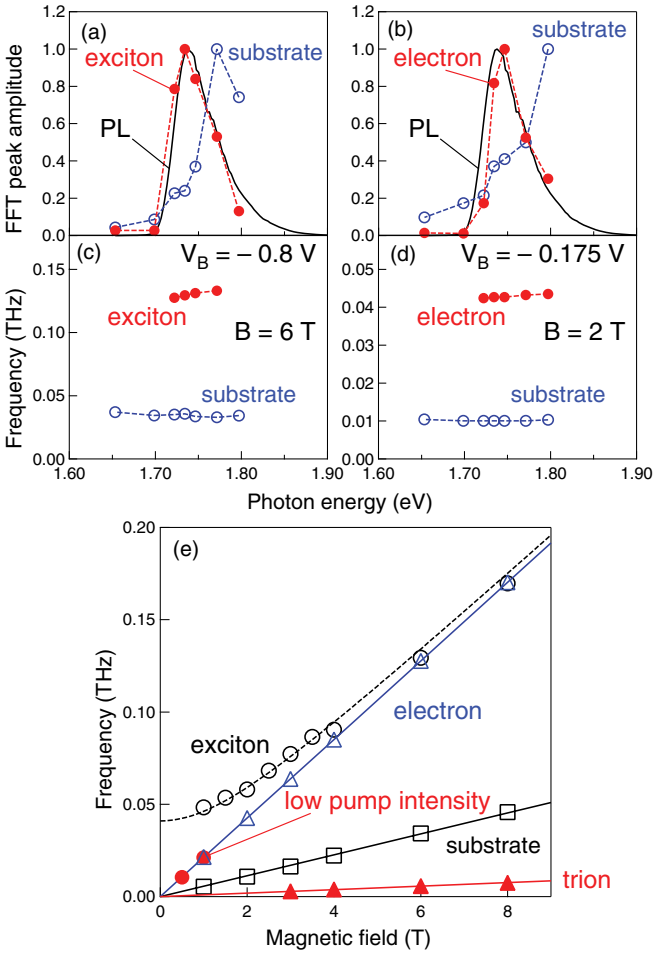


FIG. 3. (Color online) Photon energy $E_p$ dependence of the FFT amplitudes (a), (b) and frequencies (c), (d). (e) Magnetic-field dependence of the frequencies ($E_p = 1.74$ eV).

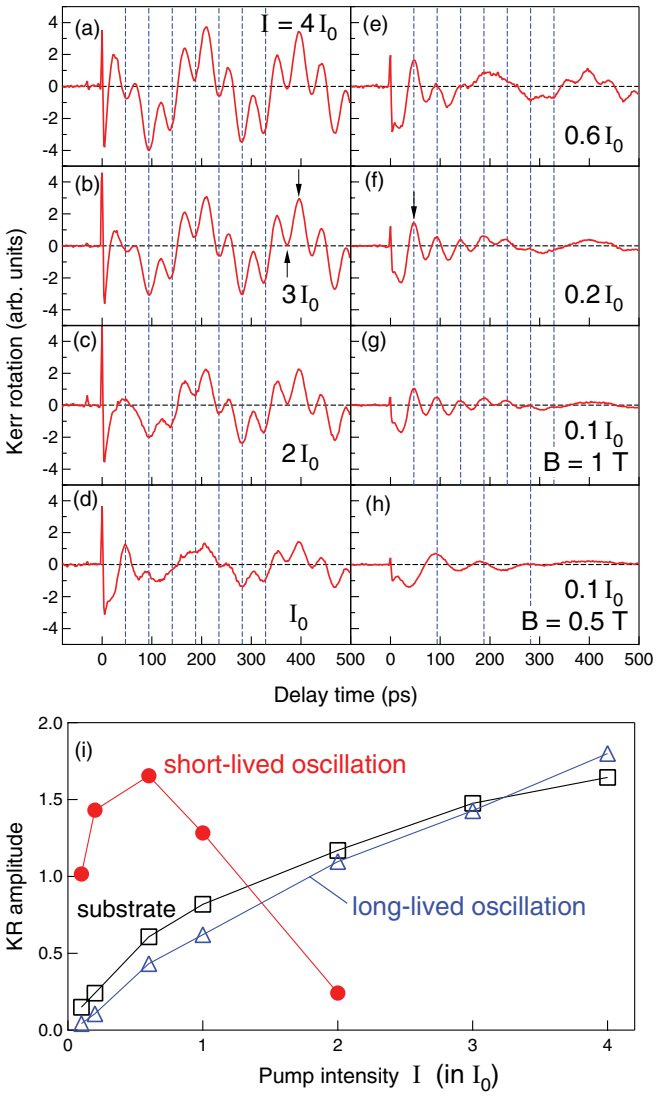


FIG. 4. (Color online) Pump-intensity $I$ dependence of TRKR of the singly charged QDs ($V_B = -0.175$ V, $I_0 = 5$ mW). $B =$ (a)–(g) 1 T and (h) 0.5 T. Here we can compare signal amplitudes in different panels. (i) Kerr rotation amplitudes as functions of $I$. The amplitude of the short-lived oscillation is estimated from the signal at 47 ps [the oscillation peak indicated by an arrow in (f)]. The amplitude of the long-lived oscillation is determined from half the difference of the signals at 372 and 395 ps [the oscillation trough and peak indicated by arrows in (b)]. The average of the two signals gives the amplitude of the substrate component.

which is about 250 ps.[19] Meanwhile, the electron component persists for much longer than 250 ps [Fig. 2(b)], as it comes from the spin coherence in the ground state.

### B. Spin polarization of QD single electrons

From now, we focus on the spin polarization of the QD single electrons. Figures 4(a)–4(g) show the pump-intensity (average power $I$) dependence of TRKR in the singly charged QDs ($V_B = -0.175$ V) at $B = 1$ T. Here the data are normalized to set the signal minimum around 94 ps to be $-4$ at the pump intensity of $I = 4I_0$ [Fig. 4(a), $I_0 = 5$ mW]. The dependence of the substrate component (period 180 ps) on $I$ is simple. We can see its amplitude increase monotonically with $I$ [Fig. 4(i), open squares]. In contrast, the electron component shows very complicated behavior. The vertical broken lines in Fig. 4 represent the oscillation period of this component (47 ps at $B = 1$ T). The time dependence is qualitatively different between the high- [Figs. 4(a) and 4(b)] and low- [Figs. 4(f) and 4(g)] intensity limits. This difference can be reduced to two points. The first is phase inversion, i.e., a discontinuous phase shift of $\pi$. The temporal points marked by the broken lines coincide with the oscillation troughs in Figs. 4(a) and 4(b), but with the peaks in Figs. 4(f) and 4(g). It appears that the spin polarization direction of the electrons is inverted simply by varying the pump intensity. The second point is the change of the oscillation lifetime which occurs along with the phase inversion. At high pump intensities [Figs. 4(a) and 4(b)], the oscillation lasts very long, as we observed earlier in Fig. 2(b) (about 2 ns). At low intensities [Figs. 4(f) and 4(g)], however, the oscillation decays extremely fast, in about 200 ps. In Fig. 4(i), we plot the Kerr rotation amplitudes of the short- and long-lived oscillations as functions of $I$ by filled circles (red) and open triangles (blue), respectively. Here we emphasize that the amplitudes of the two oscillations are not

so different. For example, the amplitude of the short-lived oscillation is 1.43 at $I = 0.2I_0$ [Fig. 4(f)]. This is close to the amplitude of the long-lived oscillation at $I = 3I_0$ [Fig. 4(b)] even though the pump intensity is 1/15. At $I = 3I_0$, we can see gradual increase of the amplitude for about 200 ps. At intermediate intensities [Figs. 4(c)–4(e)], a complicated time dependence of TRKR appears due to the competition between the high- and low-intensity features. We have not observed Rabi oscillations.[4] This may be due to the inhomogeneity of the pump power density in the probed sample area, or that of the transition dipole moments in the QD ensemble.

As the oscillation lifetimes are quite different in the two limits, we have to check whether their origins are the same. The period of the short-lived oscillation at low pump intensities coincides precisely with that of the electron component. This can be seen in Fig. 3(e), where we show the frequencies of this oscillation at $B = 0.5$ and 1 T by filled circles (red). They are obtained from the data at $I = 0.1I_0$ in Figs. 4(g) and 4(h). Here we can confirm that the oscillation period at $B = 0.5$ T is twice that at $B = 1$ T. This indicates that the exciton is not the origin of the short-lived oscillation because no influence of the electron-hole exchange $\delta$ is recognized. In addition, the exciton beat signal observed in undoped QDs [Fig. 2(a)] shows a simple linear dependence on pump intensity (not shown), where the phase inversion and the oscillation lifetime change, which characterize the data in Fig. 4, do not appear. Another possibility for the origin of the short-lived oscillation might be positively charged excitons $X^+$. They could explain the fast damping by exciton recombination, and the absence of the electron-hole exchange by pairing of holes in $X^+$. This assignment, however, cannot explain the above-mentioned large amplitude of the short-lived oscillation [Fig. 4(i)]. It is comparable to the amplitude of the long-lived electron component at high pump intensities. Therefore it is difficult to attribute the oscillation to minor species such as $X^+$. The photoexcitation of $X^+$ is possible only in positively charged QDs which are much fewer than the negatively charged ones at the voltage bias of $V_B = -0.175$ V. In addition, a change of the main feature in TRKR from $X^+$ to single electrons just by the increase of the pump intensity is unreasonable.

### C. Density-matrix calculation of spin dynamics of single electrons

In a previous paper,[20] we tried to interpret our preliminary experimental results with a standard model of the four-level system (Fig. 1). This model was based on the Hamiltonian

$$\mathcal{H} = \mathcal{H}_0 + \mathcal{V}. \tag{1}$$

Here $\mathcal{H}_0$ is the Hamiltonian of the unperturbed four-level system, and $\mathcal{V}$ is the interaction with the pump pulse in the dipole and rotating-wave approximations. Then the master equation for the density operator $\rho(t)$ was given by

$$i\hbar\frac{d}{dt}\rho(t) = [\mathcal{H},\rho(t)] + \mathcal{L}[\rho] + \mathcal{D}[\rho] + \mathcal{C}[\rho], \tag{2}$$

where we considered three relaxation processes represented by the three terms $\mathcal{L}[\rho]$, $\mathcal{D}[\rho]$, and $\mathcal{C}[\rho]$, which are described below. Our attempt was partially successful. By the density-matrix calculation, we showed that the inversion of the spin polarization direction of the electrons occurs with increase of the pump intensity when the pump pulse deviates slightly from ideal circular polarization. Eliminating other possibilities as mentioned above, we attribute the phase inversion observed in Fig. 4 to this inverted spin polarization of electrons.

The previous model, however, failed to reproduce the fast decay of the short-lived oscillation observed at low pump intensity. This and the oscillation lifetime change which accompanies the phase inversion have to be explained in the framework of the four-level system. In the previous model, three relaxation processes were taken into consideration: (A) incoherent spontaneous emission, (B) pure spin depolarization of the electron and trion, and (C) spontaneously generated coherence (SGC). The first process[21,22] (A) was represented by the term $\mathcal{L}[\rho]$ in the model, and the rate was given by the parameter $\Gamma$.[20] This term phenomenologically expresses trion recombination by incoherent spontaneous emission, which has no direct influence on the electron spin coherence [$\mathcal{L}[\rho]_{01} = 0$ (Ref. 23)]. The next process (B) was represented by the term $\mathcal{D}[\rho]$.[20] It is pure spin decoherence, whose rates were given as $\gamma_{e2}$ and $\gamma_{T2}$ for the electron and trion, respectively. These rates should be defined to reproduce the long lifetime of the electron component ($1/\gamma_{e2} = 1/\gamma_{T2} =$ 2 ns), and therefore the fast decay of the short-lived oscillation (200 ps) cannot be attributed to this process (B). The last process (C) accompanies the spontaneous emission (A), and was incorporated by the term $\mathcal{C}[\rho]$ in the model. This affects the electron spin coherence (the density-matrix element $\rho_{01}$) only when the spin precession frequency $\omega = g_e\mu_B B/\hbar$ is smaller than the trion recombination rate $\Gamma$. In the present case of InP QDs, it is not significant at $B = 1$ T. After all, the fast decay of the short-lived oscillation observed at low pump intensity could not be explained by any (or any combination) of the above three processes. Therefore we need to consider another mechanism to explain the fast decay of the oscillation.

Although the lifetime of the oscillation (about 200 ps) is close to the trion recombination lifetime, it cannot be attributed to the incoherent decay of the trion (A) which does not erase electron spin coherence even if it is accompanied by SGC (C). These processes (A) and (C) do not postulate optical coherence between the electron and trion states. But optical coherence should be generated by the pump pulse and should have a long lifetime in QDs.[11] Here we discuss the influence of the optical coherence on the electron spin dynamics quantitatively.

The optical coherence is associated with the off-diagonal elements $\rho_{ij}$ [$i = 0$ or 1, $j = 2$ or 3 (Ref. 23)], and can be represented by the mean value $\langle \boldsymbol{p} \rangle$ of the optical polarization. It has the components

$$\langle p_x \rangle = \mu(\rho_{20} + \rho_{31} + \rho_{02} + \rho_{13}) \tag{3}$$

for the $\pi_x$ and

$$\langle p_y \rangle = i\mu(-\rho_{30} - \rho_{21} + \rho_{12} + \rho_{03}) \tag{4}$$

for the $\pi_y$ direction, where $\mu$ and $i\mu$ are the transition dipole moments for the respective directions, including the phase factor. We consider the radiation emission by $\langle \boldsymbol{p} \rangle$ and its influence on the electron spin coherence. We will call this process (D) coherent spontaneous emission. To incorporate it

in the calculation model, we use a modified Hamiltonian

$$\mathcal{H} = \mathcal{H}_0 + \mathcal{V} + \mathcal{U}. \tag{5}$$

The third term $\mathcal{U}$ represents the process (D). Here we give it in the form

$$\mathcal{U} = -\boldsymbol{p} \cdot \boldsymbol{E} = -p_x E_x - p_y E_y, \tag{6}$$

where $\boldsymbol{p}$ is the optical polarization operator.[20] We assume the effective electric field $\boldsymbol{E}$ acting on the four-level system to be

$$\boldsymbol{E} = \frac{1}{6\pi\epsilon_0 c^3}\frac{d^3}{dt^3}\langle \boldsymbol{p}\rangle. \tag{7}$$

This expression for $\boldsymbol{E}$ was originally given by classical field theory to describe the so-called radiation damping of moving charged particles.[24] We obtain Eq. (7) by replacing the electric polarization in the formula with the mean value $\langle \boldsymbol{p}\rangle$. Then we use Eq. (7) to express the reaction of the radiation emission by $\langle \boldsymbol{p}\rangle$ on the four-level system. In the calculation of $\mathcal{U}$, we employ the rotating-wave approximation again. The rate of the process (D) can be controlled by a parameter $U = \mu^2\omega_T^3/3\pi\epsilon_0 c^3\hbar$.[25]

Figures 5(a) and 5(b) show the calculated time dependence of the electron spin component $\langle s_z\rangle$ along the observation axis $z$. They are for two real Rabi amplitudes $\Omega = 0.8 \times 10^{12}$ and $21 \times 10^{12}$ rad s$^{-1}$ representing the low- and high-pump-intensity cases, respectively ($B = 1$ T). They reproduce the two important features observed experimentally in Fig. 4, which are the phase inversion and the oscillation lifetime change occurring simply on variation of the pump pulse intensity $\Omega$. In particular, we stress that the fast decay of the oscillation at low pump intensity [Figs. 4(f) and 4(g)] is reproduced successfully [Fig. 5(a)]. In the calculation of Figs. 5(a) and 5(b), we assume three important parameters $U = 4 \times 10^{10}$ s$^{-1}$, $\Gamma = 5 \times 10^8$ s$^{-1}$, and $\theta = 1.02\pi/4$ (pump polarization ellipticity). We will describe the effect and meaning of the three parameters in the following.

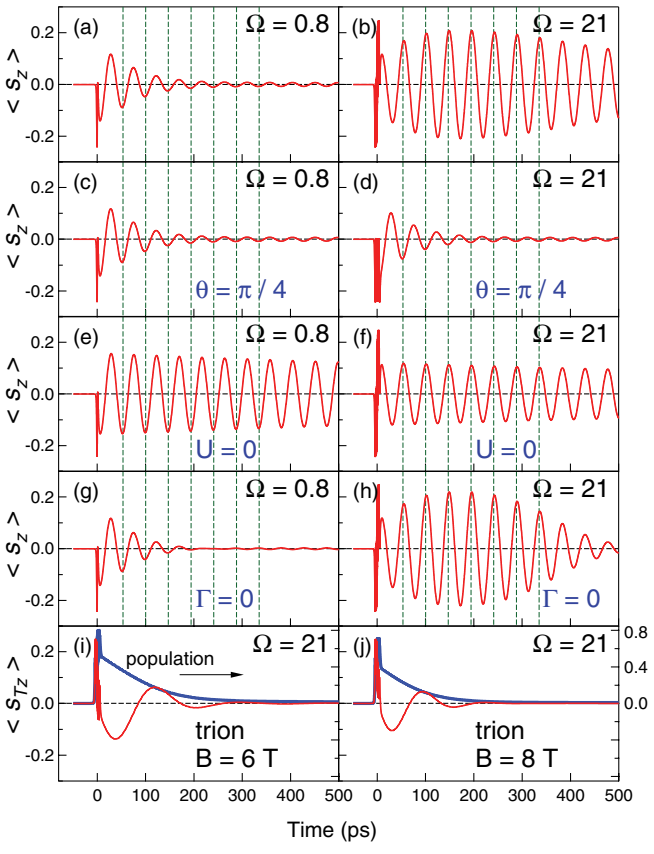


FIG. 5. (Color online) Calculated time dependence of the spin components $\langle s_z\rangle$ (a)–(h) and $\langle s_{Tz}\rangle$ [(i) and (j), thin red lines (Ref. 25)]. (a),(b) $\theta = 1.02\pi/4$, $U = 4 \times 10^{10}$ s$^{-1}$, and $\Gamma = 5 \times 10^8$ s$^{-1}$. One of these three parameters is changed in (c)–(h) as indicated in the respective panels. Broken lines (green) show the period of the electron spin precession at $B = 1$ T. Thick lines [(i) and (j), blue] show the time dependence of the trion population $\rho_{22} + \rho_{33}$ (Ref. 23). The total population is normalized to unity ($\rho_{00} + \rho_{11} + \rho_{22} + \rho_{33} = 1$).

Although the experimental pump pulse is circularly polarized, we assume its polarization ellipticity $\theta$ to be $1.02\pi/4$ in the calculation. This means outwardly that the pump pulse deviates slightly from the perfect circular polarization $\sigma^+$ ($\theta = \pi/4$). Actually, however, we assume this value to consider the optical anisotropy of the self-assembled QDs which exists in the $xy$ plane.[26] The optical anisotropy is mainly due to the anisotropic shape of the QDs with $C_{2v}$ or lower symmetry, and results in a small difference of the dipole moments $\mu$ for the $\pi_x$ and $\pi_y$ directions. As the ellipticity $\theta$ is defined here by the ratio of the Rabi amplitudes for the two directions[20] ($\tan\theta = \Omega_y/\Omega_x$), we can allow for the anisotropy of $\mu$ by a value of $\theta$ which deviates from $\pi/4$. For the ensemble of QDs, this anisotropy of $\mu$ should have inhomogeneity, and it cannot be compensated by adjustment of the light polarization. The assumption of $\theta = 1.02\pi/4$ enables the optical coupling between $|\bar{z}\rangle$ and a trion state [Fig. 1(b)]. It gives rise to the phase inversion of the oscillation in Figs. 5(a) and 5(b). As seen in Figs. 5(c) and 5(d), the inversion does not occur if we assume $\theta = \pi/4$. Therefore we ascribe the inversion observed experimentally in Fig. 4 to the optical anisotropy of the QDs.

The fast oscillation decay at $\Omega = 0.8$ [Fig. 5(a)] is due to the coherent process (D) which is represented by the parameter $U$. If we neglect its effect ($U = 0$), the fast decay disappears [Fig. 5(e)]. Meanwhile, the incoherent process (A) is the origin of the long-lived oscillation at $\Omega = 21$ [Fig. 5(b)]. If we do not consider this process ($\Gamma = 0$), the oscillation decays much faster due to the unilateral effect of the process (D) as seen in Fig. 5(h). Consequently, we attribute the fast oscillation decay (about 200 ps) observed experimentally in Figs. 4(f) and 4(g) to the coherent part of the spontaneous emission [process (D): $U$], while we attribute the slow decay (about 2 ns) observed in Figs. 4(a) and 4(b) to the incoherent part [process (A): $\Gamma$]. In general, these two types of oscillation decay coexist in our experimental data on the ensemble of QDs [Figs. 5(c)–5(e)]. This is mainly due to the inhomogeneity of the pump power density on the sample surface.

In Figs. 5(g) and 5(h) ($\Gamma = 0$), we can see that the oscillation decay by the coherent process (D) is much slower at $\Omega = 21$ than at $\Omega = 0.8$ although the same value of $U$ ($=4 \times 10^{10}$ s$^{-1}$) is assumed. The slowing down at $\Omega = 21$ makes the effect of the incoherent process (A) relatively more significant. This is the reason why the long-lived oscillation originating from the process (A) is dominant in Fig. 5(b) ($\Omega = 21$) by contrast with the data in Fig. 5(a) ($\Omega = 0.8$). The slowing down of

the oscillation decay does not occur in the case of $\theta = \pi/4$ [Fig. 5(d)] where the phase inversion is absent. Therefore we can say that it is a phenomenon peculiar to the phase-inverted cases. This explains why the phase inversion is accompanied by increase of the oscillation lifetime.

Last of all, we refer to the trion spin dynamics. Figures 5(i) and 5(j) show the time dependence of the trion spin component $\langle s_{Tz} \rangle$ calculated with the same parameters as those in Fig. 5(b), but at the magnetic fields of $B = 6$ and 8 T, respectively. They show slow oscillations for a few periods owing to the trion spin precession. This calculation result is in agreement with the experimental observation in Figs. 2(e) and 2(f). The fast oscillation damping reflects primarily the population decay of trions which is represented by thick lines (blue) in Figs. 5(i) and 5(j).

## IV. SUMMARY

In summary, we have experimentally studied the spin dynamics of excitons, electrons, and trions in charge-tunable InP/InGaP QDs excited by picosecond resonant laser pulses by means of TRKR measurements. In singly charged QDs, the inversion of the spin polarization direction of doped electrons is found to be caused simply by varyiation of the pulse intensity. It is accompanied by a change of the spin coherence time. This phenomenon is reproduced by density-matrix calculations, and explained by the competition between the coherent and incoherent parts of the spontaneous emission as the relaxation processes of the photoexcited electron-trion four-level system. This means that the optical coherence is another critical factor which influences the spin coherence. As the state of the optical polarization $\langle \boldsymbol{p} \rangle$ can be directly manipulated by light pulses, we can expect new control techniques for the electron spin dynamics by the use of the coherent part.

## ACKNOWLEDGMENT

This work was supported by Grant-in-Aid for Scientific Research No. 23340084 from the MEXT of Japan.

[1] A. Imamoğlu, D. D. Awschalom, G. Burkard, D. P. DiVincenzo, D. Loss, M. Sherwin, and A. Small, Phys. Rev. Lett. **83**, 4204 (1999).

[2] *Semiconductor Spintronics and Quantum Computation*, edited by D. D. Awschalom, D. Loss, and N. Samarth (Springer, Berlin, 2002).

[3] M. V. Gurudev Dutt, Jun Cheng, Bo Li, Xiaodong Xu, Xiaoqin Li, P. R. Berman, D. G. Steel, A. S. Bracker, D. Gammon, Sophia E. Economou, Ren-Bao Liu, and L. J. Sham, Phys. Rev. Lett. **94**, 227403 (2005).

[4] A. Greilich, R. Oulton, E. A. Zhukov, I. A. Yugova, D. R. Yakovlev, M. Bayer, A. Shabaev, Al. L. Efros, I. A. Merkulov, V. Stavarache, D. Reuter, and A. Wieck, Phys. Rev. Lett. **96**, 227401 (2006).

[5] J. R. Petta, A. C. Johnson, J. M. Taylor, E. A. Laird, A. Yacoby, M. D. Lukin, C. M. Marcus, M. P. Hanson, and A. C. Gossard, Science **309**, 2180 (2005).

[6] A. Greilich, D. R. Yakovlev, A. Shabaev, Al. L. Efros, I. A. Yugova, R. Oulton, V. Stavarache, D. Reuter, A. Wieck, and M. Bayer, Science **313**, 341 (2006).

[7] M. Atatüre, J. Dreiser, A. Badolato, A. Hogele, Khaled Karrai, and A. Imamoğlu, Science **312**, 551 (2006).

[8] J. Berezovsky, M. H. Mikkelsen, N. G. Stoltz, L. A. Coldren, and D. D. Awschalom, Science **320**, 349 (2008).

[9] D. Press, T. D. Ladd, B. Zhang, and Y. Yamamoto, Nature **456**, 218 (2008).

[10] T. A. Kennedy, A. Shabaev, M. Scheibner, Al. L. Efros, A. S. Bracker, and D. Gammon, Phys. Rev. B **73**, 045307 (2006).

[11] D. Birkedal, K. Leosson, and J. M. Hvam, Phys. Rev. Lett. **87**, 227401 (2001).

[12] I. E. Kozin, V. G. Davydov, I. V. Ignatiev, A. V. Kavokin, K. V. Kavokin, G. Malpuech, Hong-Wen Ren, M. Sugisaki, S. Sugou, and Y. Masumoto, Phys. Rev. B **65**, 241312(R) (2002).

[13] I. A. Yugova, I. Ya. Gerlovin, V. G. Davydov, I. V. Ignatiev, I. E. Kozin, H. W. Ren, M. Sugisaki, S. Sugou, and Y. Masumoto, Phys. Rev. B **66**, 235312 (2002).

[14] T. Amand, X. Marie, P. Le Jeune, M. Brousseau, D. Robart, J. Barrau, and R. Planel, Phys. Rev. Lett. **78**, 1355 (1997).

[15] I. A. Yugova, A. Greilich, E. A. Zhukov, D. R. Yakovlev, M. Bayer, D. Reuter, and A. D. Wieck, Phys. Rev. B **75**, 195325 (2007).

[16] Y. Masumoto, I. V. Ignatiev, K. Nishibayashi, T. Okuno, S. Yu. Verbin, and I. A. Yugova, J. Lumin. **108**, 177 (2004).

[17] *Semiconductors. Physics of Group IV Elements and III-V Compounds*, edited by O. Madelung, Landolt-Börnstein, New Series, Group III, Vol. 17, Pt. a (Springer, Berlin, 1982).

[18] I. V. Ignatiev, T. Okuno, S. Yu. Verbin, I. A. Yugova, and Y. Masumoto, Physica E **17**, 365 (2003).

[19] M. Ikezawa, B. Pal, Y. Masumoto, I. V. Ignatiev, S. Yu. Verbin, and I. Ya. Gerlovin, Phys. Rev. B **72**, 153302 (2005).

[20] S. Tomimoto, K. Kawana, A. Murakami, and Y. Masumoto, J. Lumin, doi: 10.1016/j.jlumin.2011.09.047.

[21] S. E. Economou, Ren-Bao Liu, L. J. Sham, and D. G. Steel, Phys. Rev. B **71**, 195327 (2005).

[22] Supplementary information in Ref. 9.

[23] The subscript numbers denoting a matrix element represent the levels in Fig. 1(a).

[24] L. D. Landau and E. M. Lifshitz, *The Classical Theory of Fields* (Pergamon, Oxford, 1975). Equation (7) assumes an electric dipole in vacuum for simplicity ($\epsilon_0$ and $c$ are the permittivity and light speed in vacuum, respectively), although the QDs are embedded in InGaP barriers.

[25] The parameters are defined in Ref. 20. We assume resonant pump pulses at $\hbar\omega_0 = \hbar\omega_T = 1.74$ eV [Fig. 1(a)] with a temporal width of 2 ps ($\kappa = \kappa_0 = 0.88 \times 10^{12}$ s$^{-1}$, $\delta = -\pi/2$). The effect of SGC (Refs. 3 and 21) is included ($\Gamma_c = \Gamma$). We assume the same rates of pure spin decoherence for the electron and trion ($1/\gamma_{e2} = 1/\gamma_{T2} =$ 2 ns).

[26] M. Sugisaki, Hong-Wen Ren, S. V. Nair, K. Nishi, S. Sugou, T. Okuno, and Y. Masumoto, Phys. Rev. B **59**, R5300 (1999).